Nonlinear acoustic waves in media with absorption and dispersion

B. B. Voronov, A. I. Korobov, and O. V. Rudenko

M. V. Lomonosov Moscow State University

Usp. Fiz. Nauk **162**, 159–176 (September 1992)

A series of laboratory exercises in nonlinear wave physics assigned to students of the Physics Department of the Moscow State University in the laboratory of the Acoustics Section is described. The series consists of three assignments: 1) experimental investigation of nonlinear waves in dissipative media; 2) Investigation of nonlinear phenomena in acoustic beams by mathematical simulation using personal computers, and 3) Experimental investigation of wave propagation in a medium with dispersion (capillary waves on the surface of a liquid). As a result of carrying out these assignments, the students become familiar with the characteristic features of the behavior of nonlinear waves and the modern methods of describing and studying them.

INTRODUCTION

The recent developments in nonlinear wave theory, and nonlinear optics and acoustics have required their inclusion in the modern education process. A number of monographs and textbooks (Refs. 1–8) has been published partly due to this reason.

We shall describe below the special practical laboratory exercises which are compulsory tasks for students graduating in radio physics in the Physics Department of Moscow State University. These exercises acquaint the students with the problems of mathematical description and physical properties in the investigation of nonlinear wave processes.[1] They are devoted to the effects of absorption, diffraction and dispersion in nonlinear wave interaction realized in acoustic media. Of course these effects are inherent not only in acoustic waves but also in waves of another physical nature. In fact the acoustic waves may be considered as a convenient objects for a simple modeling process of nonlinear wave propagation in optics, plasma physics, geophysics etc. So this allows one to give students an idea about the universal features of intense scalar wave propagation. Moreover performing of laboratory exercises enables the students to master the specific techniques of physical experiment.

Acoustic media are characterized usually by a quadratic nonlinearity and a weak dispersion so the propagation of the wave beam with axial symmetry along the x axis can be described by the evolution equation

$$\frac{\partial p}{\partial x} - \frac{\varepsilon}{c_0^3\rho_0} p \frac{\partial p}{\partial \tau} = \hat{L}p + \frac{c_0}{2}\Delta_\perp \int p \, . \tag{1}$$

Here $p(x,\mathbf{r},\tau)$ is the acoustic pressure field, ρ_0 is the mass density, ε is the media parameter of nonlinearity. It is convenient to describe the wave profile distortion using the reference frame of co-moving coordinates: $\tau = t - (x/c_0)$, here c_0 is the sound velocity. $\mathbf{r}$ are the transversal coordinates in the cross section of the beam, orthogonal to the x axis, $\Delta_\perp$ is the corresponding Laplace operator. The linear operator $\hat{L}$ describes the frequency dependent absorption and dispersion effect.[1]

Since all three effects (absorption, diffraction and dispersion) can compete with nonlinear effects the wave propagation conditions essentially depend on the interrelations between corresponding the characteristic lengths x_a, x_{df}, x_{ds} and the nonlinearity length x_n. The most interesting cases correspond to the cases when the nonlinearity is expressed strongly. Accordingly the situation should be considered when the nonlinearity length x_n is smaller then each of the three other characteristic lengths, whereas the interrelations between x_a, x_{df}, x_{ds} can be arbitrary.

The practical study of the typical cases is organized in the form of three practical assignments for students in the Acoustics Section. Two of them use experimental apparatus while the third one is realized as a mathematical simulation using a personal computer.

1. EXPERIMENTAL STUDY OF NONLINEAR WAVES IN DISSIPATIVE MEDIA[1)]

For plane waves in dissipative media we take the situation when the diffraction and dispersion processes are negligible: $x_{df} \to \infty$ and $x_{ds} \to \infty$. The mathematical description of such waves is based on the Bürgers equation[1,3]

$$\frac{\partial U}{\partial x} = \frac{\varepsilon}{c_0^2} U \frac{\partial U}{\partial \tau} + \frac{b}{2c_0^3\rho_0}\frac{\partial^2 U}{\partial \tau^2}, \tag{1.1}$$

which follows from Eq. (1) $p = p(x,\tau) = \rho_0 c_0 U$, $\hat{L} = (b/2c_0^3\rho_0)\partial^2/\partial\tau^2$, where U is the particle vibration velocity, b is the effective dissipation parameter (for water $b = 4\cdot 10^{-2}$ P, the nonlinear parameter $\varepsilon = 3.5$–4, $c_0 = 1480$ m/s. Such a form of the dissipative term $\hat{L}$ is typical for acoustics where viscous and thermoconductive absorption terms are usually proportional to f^2 where $f = \omega/2\pi$.

In nondispersive media during the initial (frequency ω) signal propagation a synchronous generation of higher harmonics 2ω, 3ω ... takes place (the number of harmonics $n \approx x_n/x_a \gg 1$) and the wave profile $U(\tau)$ is progressively distorted as the distance x traveled by the wave increases up to shock wave formation at $x = x_s$ (x_s is the shock wave formation length).

For large Reynolds numbers $\mathrm{Re} = c_0\rho_0 U_0/b\omega \gg 1$ the wave profile distortion is similar to the process in an ideal liquid up to $x = x_s$. In this case the profile distortion process is described by the Riemann wave equation

 0038-5670/92/090796-09$03.00

$$\frac{\partial U}{\partial x} - \frac{\varepsilon}{c_0^2} U \frac{\partial U}{\partial \tau} = 0, \tag{1.2}$$

which follows from Eq. (1.) for $b = 0$.

The Riemann solution of Eq. (1.2) in terms of x, t for $U\varepsilon/c_0 \ll 1$ and the boundary condition $U(x = 0,t) = U_0 \sin \omega t$ is[1-4]

$$U = U_0 \sin\left[\omega\left(\tau + \frac{\varepsilon}{c_0^2} U x\right)\right] = U_0 \sin\left\{\omega\left[t - \frac{x}{c_0(1 + \varepsilon U c_0^{-1})}\right]\right\}. \tag{1.3}$$

It follows from Eq. (1.3) that the wave sectors having different particle velocities U propagate with different velocities $c_0 + \varepsilon U$, when $U > 0$ the wave velocity is supersonic, when $U < 0$ it is subsonic. Therefore a distortion of the initial wave profile is developing. For small Mach numbers $\mathrm{Ma} = U/c_0 \ll 1$ (in liquids typical Mach numbers are of the order of 10^{-3}–10^{-4} (Refs. 1–6, 8) wave profile distortions are negligible at distances comparable with the wavelength λ. However these weak distortions have a cumulative character, i.e., nonlinearity leads to significant distortions at large distances. This fact is typical for nondispersive media.

Equation (1.3) allows one to illustrate the evolution of the wave profile in a simple way by means of a graphical analysis.

In the case $\mathrm{Ma} \ll 1$ the spatial form of the initial wave near the source will reproduce the temporal one i.e. for $U(0,t) = U_0 \sin \omega t$

$$U(x) = U_0 \sin(2\pi x/\lambda). \tag{1.4}$$

After the time interval $t_1 \gg 2\pi/\omega$ those points of the profile for which $U = 0$ will be shifted to the distance $x_1 = c_0 t_1$, the other points ($U \neq 0$) will be shifted to the distance

$$x = (c_0 + \varepsilon U) t_1,$$

i.e., the relative shift between points for which $U \neq 0$ and $U = 0$ will be

$$\Delta x = \varepsilon U t_1 = \varepsilon x_1 U/c_0 = \varepsilon \mathrm{Ma} x_1. \tag{1.5}$$

The new wave form (after a time t_1) can be obtained by the addition of x_1 shift to the initial sine curve along the abscissa axis. It is convenient for the construction of the profile to draw the straight line $U = kx$ where $k = c_0/\varepsilon x_1$ (see Fig. 1a) and to shift each profile point by the corresponding value.

It is clear from this graphical analysis that the nonlinear distortions have a cumulative character: the forward front of the positive half-period becomes steeper and the back front becomes flatter the larger is the wave path x_1. At a certain distance at the point at which $U = 0$ a discontinuity in the wave profile occurs. This distance x_s which has the meaning of the nonlinearity length x_n can be obtained from the equality of the slope angle of the $U = kx$ straight line and of the sine curve $U = U_0 \sin(2\pi x/\lambda)$ for $U = 0$: $\partial U/\partial x|_{Y=0} = k$ or $U_0 \cdot 2\pi/\lambda = c_0/\varepsilon x_p$, therefore

$$x_p = \frac{c_0^2}{\varepsilon \omega U_0} = \frac{\lambda}{2\pi\varepsilon \mathrm{M}} = \lambda N_\lambda, \tag{1.6}$$

where $N_\lambda = (2\pi\varepsilon \mathrm{M})^{-1}$ is the number of wavelengths between $x = 0$ and the point of shock wave formation. The N_λ value depends on the media properties which are determinated by the parameter ε and the initial disturbance value U_0.

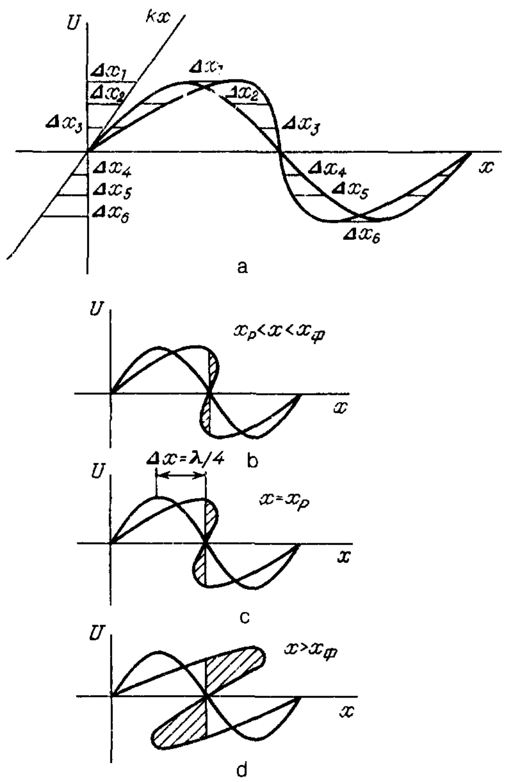

FIG. 1. Graphical analysis of the nonlinear deformation of a simple wave profile.

If one continues this procedure at distances $x > x_s$ a multivalued solution of the equation $U(x) = 0$ arises (see Fig. 1 b–d). In real dissipative media this can not occur. The presence of even arbitrarily low losses leads to a significant dissipation of energy along the steep sections of the waves. Instead of the wave "overturning" a wave front of a small but finite width Δ appears. The relative width of this front is

$$\delta = \frac{\Delta}{\lambda} = \frac{1 + (\varepsilon \omega M_0 x/c_0)}{\pi \varepsilon \mathrm{Re}} \tag{1.7}$$

and $\delta \ll 1$ for $\mathrm{Re} \gg 1$.

Therefore for determining the wave profile at distances $x \geqslant x_s$ we can continue our graphic construction neglecting the wave front width but retaining only those parts of the wave which do not go beyond the boundaries of the discontinuity (see Fig. 1b). The part of the wave energy corresponding to the shaded areas is absorbed by the medium.

It follows from Fig. 1 that at the discontinuity the difference of velocity will increase and when it reaches the maximum value $2U_0$ the wave will take on a sawtooth form. The corresponding distance is referred to as the "forming" distance x_f. It can be determined using Eq. (1.5) and the condition $\Delta x|_{u = u_0} = \lambda/4$ (see Fig. 1c),

$$x_{(f)} = \frac{\lambda}{4\varepsilon \mathrm{M}} = \frac{\pi}{2} x_p. \tag{1.8}$$

With the further shock wave propagation the velocity discontinuity will decrease (see Fig. 1d). It is easy to show that at the distance $x_1 = \pi \rho c_0^3 / 2b\omega^2$ from the source with $U = U_0 \sin \omega t$ the acoustic wave becomes almost sinusoidal and its amplitude does not exceed $U_0' = \omega b \epsilon / \rho_0 c_0$, at $x > x_1$ the wave amplitude does not depend on its initial value and is determined only by the wave frequency and by the parameters of the medium; it is the so-called "nonlinear saturation" effect.[2,3]

The transformation of the initial sinusoidal wave into the shock one is equivalent to the production of higher harmonics in the initial wave spectrum.

The solution of Eq. (1.3) for $x < x_s$ can be written as follows[1-3]

$$\frac{U}{U_0} = \sum_{n=1}^{\infty} B_n(z) \sin\left[n\omega\left(t - \frac{x}{c_0}\right)\right], \tag{1.9}$$

where $B_n(z) = 2J_n(nz)/nz$, $z = \varepsilon\omega Ux/c_0^2$, J_n is the Bessel function of the order n. The solution (1.9) is usually referred to as the Bessel-Fubini formula and allows us to trace the dependence of the amplitudes of the harmonics on the distance $x < x_s$ (see Fig. 2).

The block diagram of the apparatus for the experimental investigation of the propagation of plane waves in dissipative media is shown in Fig. 3. The plane waves are generated by the power (up to $2.5 \cdot 10^3$ W) provided by the pulse generator *1*. Radio frequency 1 MHz pulses are applied to the quartz electromechanical transducer *2* which is fixed to the end of the special bath *8* filled with water. Both the amplitude and the length of the rf pulses can be varied by switches placed in the front panel of the generator *1*. The bath construction enables establishing the plane wave regime without any reflection from the opposite end of the bath.

The receiving X-cut quartz plate-with the resonance frequency of 10 MHZ was attached to the special device traveling along the wave propagation direction during the measurements. The amplitude-phase characteristic of the receiver is almost constant up to 10 MHz therefore the fundamental frequency signal as well as the signals of higher (up to $n = 10$) harmonics can be received and also the time profile of the plane wave can be registered. The diameter of the receiver is equal to $10\,\lambda$ of the initial wavelength therefore the received signal is averaged over the cross section area of the quartz plate. The received signal is directed to the wide-band oscilloscope *4* and simultaneously to the spectrum analyzer *5* so the wave profile and the spectrum evolution as a function of the wave path can be observed (see Fig. 4). The fast oscillation in the beginning of the positive half-$\pm$ period of the plane wave at $x \gg x_s$ is caused by the appearance in the signal spectrum of the 10th harmonics coincident with the receiving plate eigen oscillations.

The wave intensity 1 is measured by the calorimeter *6* with the electrical thermometer *7* which are removed from

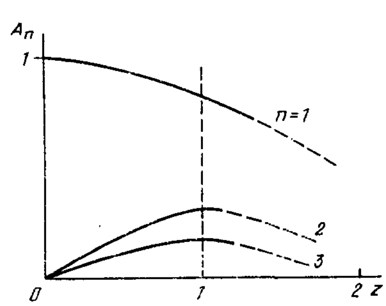

FIG. 2. The first, the second and the third harmonic amplitudes curves for $\mathrm{Re} \gg 1$ as functions of the distance.

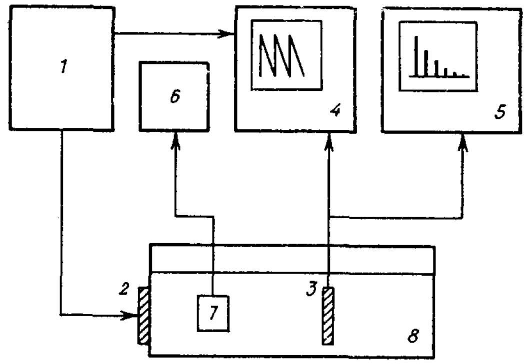

FIG. 3. The block diagram of the experimental apparatus for studying plane waves in a dissipative medium.

the bath before the main experiment. From the known intensity the amplitudes of the excess wave pressure $p_0 = (2\rho_0 c_0 I)^{1/2}$ and of the particle velocity $U_0 = (2I/\rho_0 c_0)^{1/2}$ were calculated and the acoustic Reynolds number $2\varepsilon \cdot \mathrm{Re}$ was determined where $\mathrm{Re} = p_0/b\omega$. Students had to measure experimentally the discontinuity length x_s and the sawtooth formation length x_f, to construct graphically the wave profile at these points (see Fig. 1) and to compare the theoretical data with the experimental ones (see Figs. 2 and 4).

The bath length in the wave propagation direction was too small to observe the dissipative smoothing out of the sawtooth wave into a sinusoidal one so the influence of the dissipative processes was studied at small Reynolds numbers $\mathrm{Re} \ll 1$; when the nonlinear term in Eq. (1.1) is negligible this equation can be solved by the method of successive approximations.

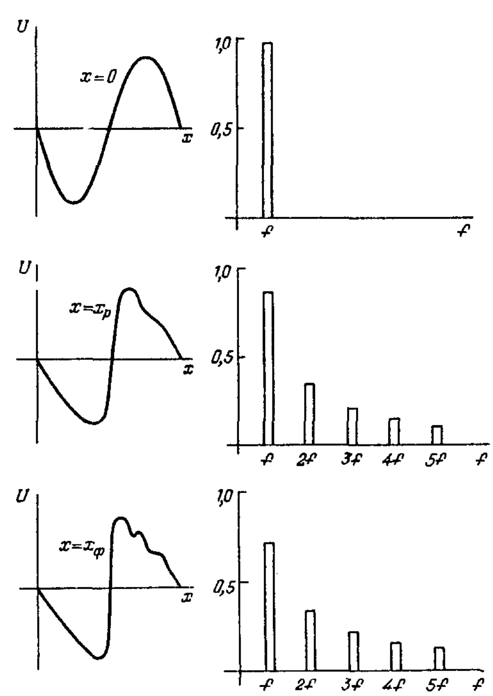

FIG. 4. Experimental oscillograms of the wave profile (a) and the wave spectrum (b) for different distances.

With the boundary condition $U_{2\omega}(x=0)=0$ corresponding to the absence of the second harmonic at the input into the system the solution of Eq. (1.1) can be written as

$$U_{2\omega}=\frac{\varepsilon U_0 \mathrm{Re}}{2}[\exp(-2\alpha x)-\exp(-4\alpha x)]\sin 2\omega\tau, \tag{1.10}$$

where $\alpha=b\omega^2/2c_0^3\rho_0$ is the wave absorption coefficient which depends on the frequency. Figure 5 shows the curve which illustrates the ratio $U_{2\omega}/U_0$ as a function of x. The amplitude of the second harmonic increases initially according to a linear law because of the nonlinear pumping of energy from the wave of the initial frequency, and then begins to fall off due to the predominant effect of dissipative processes.

For the experimental observation of this process the radiated power was decreased to a value such that the wave profile was distorted during the wave propagation but the discontinuity did not appear. The experimental dependence of the second harmonic amplitude on the wave path measured with the use of the spectrum analyzer was compared with the theoretical curve (see Fig. 5).

The experimental device parameters were chosen to correspond to the nondiffractional case of wave propagation so that the plane wave approximation could be used in the calculations.

2. INVESTIGATION OF ACOUSTIC BEAM NONLINEAR PROPERTIES BY MATHEMATICAL SIMULATION USING A PERSONAL COMPUTER[2)]

In the previous section we considered only one-dimensional waves. In real cases we must consider the bounded sound beams with a non-negligible aperture value. Accordingly diffraction effects must be taken into account. In order to study nonlinear effects in acoustic beams it is useful to neglect the influence of absorption ($x_a\to\infty$) and dispersion ($x_{ds}\to\infty$). This corresponds to $\hat{L}=0$ in Eq. (1) and we obtain the Khokhlov–Zabolot-skaya (KZ) equation[1] which describes wave propagation including diffraction and nonlinear effects

$$\frac{\partial}{\partial\tau}\left(\frac{\partial p}{\partial x}-\frac{\varepsilon}{c^3\rho_0}p\frac{\partial p}{\partial\tau}\right)=\frac{c_0}{2}\Delta_\perp p. \tag{2.1}$$

The wave profile distortion described by the KZ equation (2.1) results from nonlinearity and diffraction. It should be noted that in contrast to the Bürgers equation no exact solutions of the KZ equation which are of physical interest are known. Therefore special limiting cases will be considered.

If we neglect diffraction i.e., set $\Delta_\perp p=0$, Eq. (2.1) is transformed into the equation for simple waves, the solution of which (the Riemann solution) was completely analyzed in the previous section.

In another special case when the nonlinear term in Eq. (2.1) is neglected, i.e., $\varepsilon=0$, we have

$$\frac{\partial^2 p}{\partial x\,\partial\tau}=\frac{c_0}{2}\Delta_\perp p. \tag{2.2}$$

For the sinusoidal signal of the form $p=A(x,r)\cdot\exp(-i\omega\tau)$ Eq. (2.1) can be transformed into the parabolic equation of diffraction well known in wave theory[1]

$$-2ik\frac{\partial A}{\partial x}=\frac{\partial^2 A}{\partial r^2}+\frac{1}{r}\frac{\partial A}{\partial r} \tag{2.3}$$

the solution of which can be written in the form

$$A=\frac{p_0}{1+i(x/x_{\text{дф}})}\exp\left[-\frac{r^2/a^2}{1+i(x/x_{\text{df}})}\right], \tag{2.4}$$

assuming a Gauss-type boundary condition: $A(x=0,r)=p_0\exp(-r^2/a^2)$. Here

$$x_{\text{df}}=\frac{ka^2}{2}=\frac{\omega a^2}{2c_0} \tag{2.5}$$

is the characteristic diffraction length (see Fig. 6). At distances $x\gg x_{\text{df}}$ the beam with an initial plane front is transformed into a spherical wave which is concentrated within a cone of angle $\theta_{\text{df}}=\lambda/\pi a$.

Using the solution (2.4) of the parabolic equation (2.3) one can obtain the solution of the linear problem of the diffraction of a sinusoidal signal

$$\frac{p}{p_0}=\left(1+\frac{x^2}{x_{\text{df}}}\right)^{-1/2}\exp\left[-\frac{r^2/a^2}{1+(x^2/x_{\text{df}}^2)}\right]$$
$$\times\sin\left[\omega\tau+\operatorname{arctg}\frac{x}{x_{\text{df}}}-\frac{r}{a^2}\frac{x/x_{\text{df}}}{1+(x^2/x_{\text{df}}^2)}\right]. \tag{2.6}$$

Equation (2.6) enables one to follow the wave phase change along the beam axis ($r=0$)

$$\varphi=\omega\tau+\operatorname{arctg}\frac{x}{x_{\text{df}}}. \tag{2.7}$$

The main result of Eq. (2.7) is: the phase velocity of acoustic wave propagation depends on frequency and is somewhat greater than the plane wave phase velocity c_0. This is easy to see in the case $x\ll x_{\text{df}}$ when $\operatorname{arctg}(x/x_{\text{df}})\approx x/x_{\text{df}}$ and Eq. (1.6) becomes

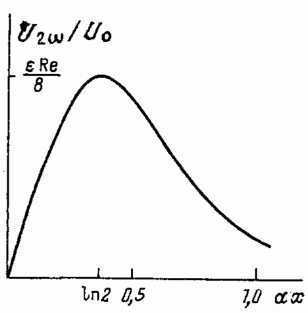

FIG. 5. The second harmonic amplitude curve as a function of distance for Re < 1.

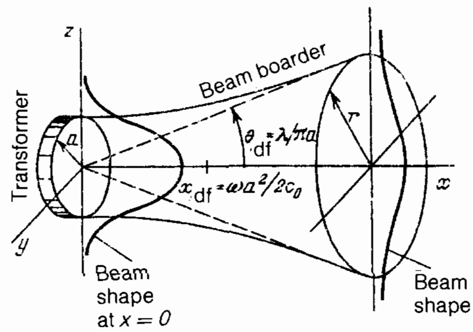

FIG. 6. The shape of an acoustic beam subject to diffraction.

$$\varphi \approx \omega\left(t-\frac{x}{c_0}\right)+\frac{2c_0}{\omega a^2}x=\omega\left(t-\frac{x}{c(\omega)}\right), \tag{2.8}$$

where $c(\omega) = c_0\cdot(1-2(c_0/\omega a)^2)^{-1}$.

It follows from Eq. (2.8) that as the frequency increases ($\omega \to \infty$) the diffraction effects become weaker and $c(\omega) \to c_0$. The diffraction shift of the phase (2.7) corresponds to the transformation of the plane wave into the spherical one described by Eq. (2.6). This transformation is easily observes at distances from $x = 0$ up to several x_{df}.

We consider now the general situation described by the KZ equation when both nonlinearity and diffraction are included. We shall take into account only two phenomena: the distortion asymmetry of the compression and rarefaction half-periods of the periodical acoustic signal and the beam isotropization effect.

The asymmetry is connected with the nonlinear effect of higher harmonic generation and the diffraction shift of phases (2.7), in other words with the small difference of phase velocity $c(\omega)$ of the different harmonics (2.8). A qualitative explanation of the asymmetric distortion of the half-periods is given by Fig. 7. For simplicity we will take into account only the two first harmonics: the initial frequency ω and the second harmonic 2ω. It follows from Eq. (2.8) that the wave velocity excess over c_0 is less the greater is the frequency. Hence the second harmonic appearing in nonlinear media has a phase shift relative to the phase of the initial frequency wave. The resulting wave profile is the sum of the two harmonic components. The profile is distorted as follows: the positive half-period is shorter than the negative one. The areas of the half-periods must be equal because of the momentum conservation law. Therefore at distances $x \approx x_{df} \approx x_s$ the positive pressure amplitude exceeds the initial value p_0. This conclusion will be valid also if a greater number of harmonics is taken into account.

The isotropization effect is connected with the nonlinear damping of discontinuities. We recall that even in ideal nonviscous media at $x < x_s$ distances (see section 1) this damping may be essential. Nonlinearity causes a decrease of the sawtooth wave "amplitude;" this decrease strongly depends on the amplitude and therefore depends on r. Nonlinear damping will be greater near the axis of the beam where the disturbance is greater. Hence the smoothing of the beam shape and of the details of the transverse field distribution will occur (see, for example, Fig. 8a, for distances $x > x_s$).

The smoothing of the transverse distribution of the field in the radial coordinate r means that the angular distribution of the field (for small angles $\theta \approx r/x$ between the beam axis and the direction to the point of observation) will also be

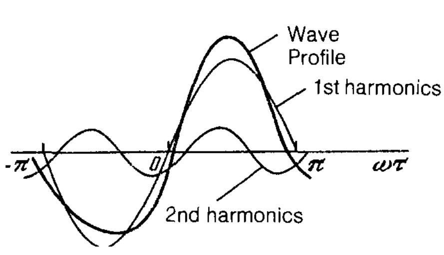

FIG. 7. The nonsymmetrically distorted wave profile (3) as a result of the sum of the initial wave (1) and the second harmonic (2).

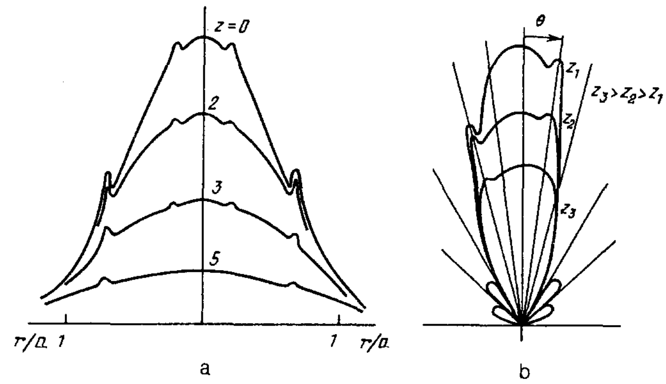

FIG. 8. The smoothing of the beam shape (a) and the isotropization of the directivity diagram (b) as a result of nonlinear damping.

smoothed out, that is isotropization of the directional pattern of radiation will occur (see Fig. 8b). A similar process is typical for parametric underwater antennas.[5,6]

The experimental investigation of nonlinear diffraction effects under laboratory conditions is connected with certain difficulties. Therefore this practical laboratory work is based on the mathematical simulation of the processes described by the KZ equation using a personal computer.

To solve the KZ equation using a computer, it is convenient to bring Eq. (2.1) to a dimensionless form. Let the acoustic field at the source be a Gaussian beam and a monochromatic signal:

$$p(x=0,r,\tau)=p_0\exp(-r^2/a^2)\sin\omega\tau, \tag{2.9}$$

where a, ω and p_0 are characteristic values of the beam width, the wave frequency and the wave amplitude respectively.

The new dimensionless variables in Eq. (2.1) are

$$\Pi=\frac{p}{c_0^2\rho_0},\quad \theta=\omega\tau,\quad R=\frac{r}{a},\quad z=\frac{x}{x_p}=\frac{\varepsilon}{c_0^3\rho_0}\omega p_0 x, \tag{2.10}$$

in terms of which Eq. (2.1) takes the form

$$\frac{\partial}{\partial\theta}\left(\frac{\partial\Pi}{\partial z}-\Pi\frac{\partial\Pi}{\partial\theta}\right)=\frac{N}{4}\left(\frac{\partial^2\Pi}{\partial R^2}+\frac{1}{R}\frac{\partial\Pi}{\partial R}\right). \tag{2.11}$$

Here $N = x_n/x_{df}$ is the ratio of the characteristic nonlinearity length x_n [see Eq. (1.6)] to the diffraction length x_{df} [see Eq. (2.5)].

The physical meaning of the number N can be understood by estimating the relative contribution of the diffraction and the nonlinear terms to Eq. (2.1)

$$\frac{(c_0/2)\Delta_\perp p}{(\varepsilon/c_0^3\rho_0)\partial(p\partial p/\partial\tau)/\partial\tau}\approx\frac{(c_0/2)p_0/a^2}{(\varepsilon/c_0^3\rho_0)p_0^2\omega^2}=\frac{c_0^4\rho_0}{2\varepsilon\omega^2a^2p_0}=\frac{N}{4}. \tag{2.12}$$

For $N \gg 1$ the diffraction term is predominant and for $N \ll 1$ the nonlinear term prevails. For example at $N = 10$ we have almost a linear problem up to distances $z \approx 10$. In this case the nonlinear term in the KZ equation is negligibly small and with good accuracy the solutions of the KZ equation correspond to the solutions of the linear equation (2.2). In particular for the sinusoidal input signal (2.9) we have the solution (2.6). For the small values $N \ll 1$ the solution to the KZ equation coincides with the Riemann simple waves solution for $z \ll 1$. For larger z we have to remove the nonuniqueness of the wave profile by drawing a discontinuity according to the law of "equality of areas."

A mathematical simulation of the KZ equation in the form (2.11) under the conditions (2.9) at $z = 0$ which in dimensionless variables has the form

$$\Pi(z = 0, R, \theta) = \exp(-R^2)\sin\theta \tag{2.13}$$

is performed using a personal computer. The direct integration of the problem (2.11), (2.13) performed with the specially elaborated net methods[9] using the powerful modern computers required heavy expenditure of machine time. This is unacceptable for student laboratory exercises. So asymptotic methods of solving the KZ equation were proposed in Ref. 10 which enable one to calculate the wave profile, the amplitude and the phase spectrum as functions of the dimensionless parameters with the use of personal computers within a few seconds.

Students have a possibility to input the initial parameters N, z, R and to observe different situations arising with the nonlinear beam propagation. As a result of programmed calculations for certain N, z, and R there appear on a display the patterns of the wave profile, the amplitude spectrum and a table of numerical values of amplitudes and phases of the first ten harmonics of the beam, as well as the asymmetry characteristics of the wave profile. Then if necessary the experimental results are printed out on a matrix printer (see Fig. 9).

The profile and the amplitude spectrum of one period of the distorted wave which has the initial sinusoidal time form at $x = 0$ is given in Fig. 9a. The parameter $N = 0$ corresponds to the nondiffracting wave with a plane front. The results relate to the space point $R = 0$, $z = 1$, i.e., the observation point is placed on he beam axis at a distance $x = x_s$ from the source. At the point $x = x_s$ a discontinuity arises and the tangent to the wave profile at $\tau = 0$ ($\theta = 0$) becomes vertical. The numerical values of the harmonics amplitudes correspond to the Bessel–Fubini formula [see Eq. (1.9)].

The same profile is represented in Fig. 9b but at a distance $z = 3$ ($x = 3x_s$). Here the nonuniqueness of the profile at the point $\tau = 0$ ($\theta = 0$) was replaced by a discontinuity according to the law of "equality of areas."[1] One can see that a sawtooth wave has been formed by straight-line parts of the smooth profile of the simple Riemann wave separated by shock fronts. The amplitude of harmonics with numbers m and n are related as $A_m/A_n \approx n/m$.

Figures 9c–d illustrate the simultaneous influence of both the nonlinear and the diffraction processes. For the sake of comparison the wave profile at $R = 0$, $z = 1.5$, $N = 0$ (the case of diffraction switched off) is represented in Fig. 9c and the wave profile at $N = 1.5$ ($x_{\rm df} = 1.5x_s$) is represented in Fig. 9d. One can see that the diffraction phase shifts between different harmonics lead to the nonsymmetrical distortion of the compression and rarefaction parts in every period of the signal.

By varying the parameter R while the parameter N and z remain fixed we have the opportunity to investigate the transverse amplitude profile of the beam, the isotropization effect, and the amplitude profiles of different harmonics.

3. EXPERIMENTAL STUDY OF SOUND WAVE PROPAGATION IN A MEDIUM WITH DISPERSION (CAPILLARY WAVES ON A LIQUID SURFACE)[3]

The third practical laboratory exercise is devoted to the properties of nonlinear waves in dispersive media and is based on an experimental study of propagation of capillary waves on a water surface.

Oscillations of a disturbed free surface of a liquid are caused by two kinds of relaxation forces: gravity and surface tension. In the case of deep water $h \gg \lambda$ (here h is the depth) the corresponding dispersion relation is the following:[1]

$$\omega^2 = gk + (\sigma k^3/\rho_0), \tag{3.1}$$

where $g = 9.8\ \mathrm{m/s^2}$ is the acceleration due to gravity, σ is the surface tension coefficient, and ρ_0 is the mass density. We note that the value of σ depends strongly on the purity of the water surface and can be about 15–20% less for nondistilled water.

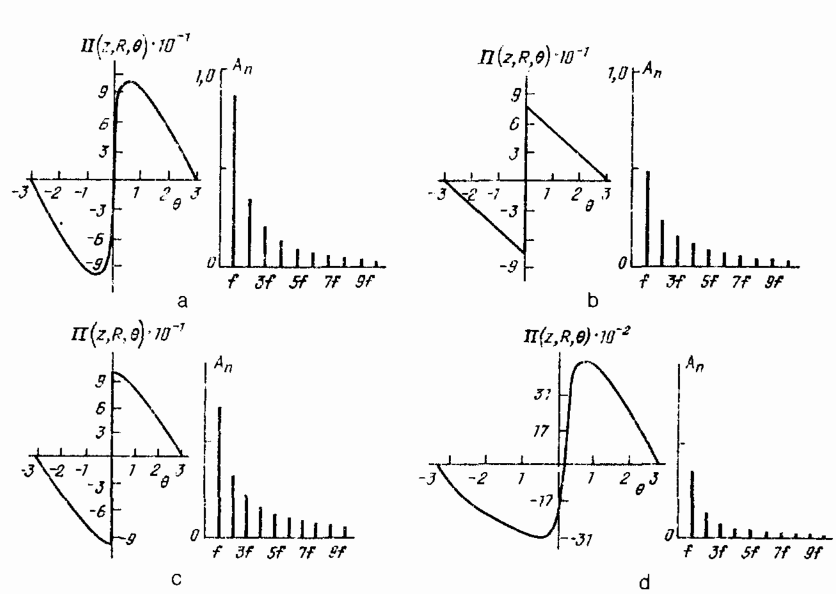

FIG. 9. The waves profiles and their spectra (on the right) for different z and N for $R = 0$. a—$z = 1$, $N = 0$. b—$z = 3$, $N = 0$. c—$z = 1.5$, $N = 0$. d—$z = 1.5$, $N = 1.5$.

The phase velocity of surface sound waves is [see Eq. (3.1)]:

$$V_{\text{ph}}=\frac{\omega}{k}=\left(\frac{\sigma k}{\rho_0}+\frac{g}{k}\right)^{1/2}=\left(\frac{g\lambda}{2\pi}+\frac{2\pi\sigma}{\rho_0\lambda}\right)^{1/2}. \qquad (3.2)$$

The frequency dependence of the phase velocity $V_{\text{ph}}(f)$ in Fig. 10 corresponds to distilled water ($\sigma=7\cdot10^2$ N/m^2, $\rho_0=10^3$ kg/m. At

$$f=\frac{1}{\sqrt{2}\pi}\left(\frac{\rho g^3}{\sigma}\right)^{1/4}$$

the velocity $V_{\text{ph}}(f)$ has a minimum: $V_{\text{ph min}}=(4\sigma g/\rho_0)^{1/4}$ and the corresponding wavelength is $\lambda_{\min}=(\sigma g/\rho_0)^{1/4}$. For distilled water $f_{\min}=13.5$ Hz, $V_{\text{ph min}}=0.235$ m/s, $\lambda_{\min}=1.73\cdot10^{-2}$ m.

For short (capillary) waves $f(\geqslant f_{\min})$ the force of surface tension prevails and the first term in Eq. (3.1) becomes negligible, so

$$\omega^2=\frac{\sigma}{\rho_0}k^3,\ V_{\text{ph}}=\frac{\omega}{k}=\left(\frac{\sigma}{\rho_0}k\right)^{1/2}=\left(\frac{\sigma}{\rho_0}\omega\right)^{1/3}, \qquad (3.3)$$

$$V_{\text{gr}}=\frac{\partial\omega}{\partial k}=\frac{3}{2}\frac{\sigma k^2}{\omega}=\frac{3}{2}V_{\text{ph}},$$

where V_{gr} is the wave group velocity.

For long (gravity) waves for $f<f_{\min}$ the second term is dominant i.e.:

$$\omega^2=gk,\quad V_{\text{ph}}=\frac{\omega}{k}=\left(\frac{g}{k}\right)^{1/2},\quad V_{\text{gr}}=\frac{\partial\omega}{\partial k}=\frac{1}{2}V_{\text{ph}}. \qquad (3.4)$$

For $f\approx f_{\min}$ both terms are of the same order: it is the case of mixed gravity-capillary waves.

The group velocity of gravity waves is less then the phase velocity. On the other hand the phase velocity of capillary waves is less then the group velocity, and anomalous dispersion occurs (see Fig. 10).

The presence of dispersion causes the essential difference in nonlinear effects in dispersive and nondispersive cases (see for example section 1), the phase velocities of different harmonics are different and phase relations between harmonics change rapidly as they propagate in space. Because of the absence of phase synchronism there is no accumulation of nonlinearity and we have no essential distortion of the wave profile.

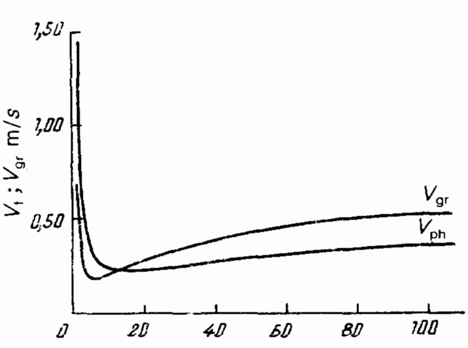

FIG. 10. The phase velocity V_{ph} and the group velocity V_{gr} of waves on the surface of water as functions of the frequency f.

The description of the acoustic field in a dispersive medium directly in terms of Eq. (1) is no longer suitable. More convenient is the equivalent description in terms of the equation for the slowly varying complex amplitudes of the quasi-harmonic components of the acoustic field. In particular, if the dispersion is such that only the first and the second harmonics can exchange energy effectively one should set in Eq. (1)

$$p(x,\tau)=\frac{1}{2}A_1\exp(i\omega\tau)+\frac{1}{2}A_2\exp(i\cdot2\omega\tau)+\text{c.c.}$$

Then if the energy dissipation is negligible, Eq. (1) is equivalent to the pair of truncated equations:[1]

$$\frac{\partial A_1}{\partial x}=-i\gamma A_1^*A_2\exp(-ix\Delta k), \qquad (3.5)$$

$$\frac{\partial A_2}{\partial x}+\hat{U}\frac{\partial A_2}{\partial\tau}=-\gamma A_1^2\exp(ix\Delta k).$$

Here A_1 and A_2 are the initial wave and the second harmonic amplitudes respectively, $\hat{U}=V_{\text{gr}}^{-1}(2\omega)-V_{\text{gr}}^{-1}(\omega)$ is the group velocity discrepancy,

$$\Delta k=k_2(2\omega)-2k_1(\omega)=\frac{2\omega}{V_{\text{ph}}(2\omega)}-2\frac{\omega}{V_{\text{ph}}(\omega)} \qquad (3.6)$$

is the wave number difference, and γ is the effective constant of nonlinearity for the surface waves.

The pair of equations (3.5) describes the main features of the second harmonic generation. The absence of the second harmonic at $x=0$ implies the boundary condition:

$$A_1(0)=A_0,\quad A_2(0)=0. \qquad (3.7)$$

We consider now the second harmonic generation in a continuous regime under the condition $|A_2|\ll|A_1|$. Then according to the first of equations (3.5) the initial wave amplitude is constant $A_1(x)\approx A_0$. If also one puts $U=0$, the second harmonic is generated in the presence of the given field of the initial wave and the pair of equations (3.5) is replaced by the equation

$$\frac{\partial A_2}{\partial x}=-\gamma A_0^2\exp(ix\Delta k). \qquad (3.8)$$

So integrating (3.8) we obtain

$$A_2=\frac{\gamma A_0^2}{\Delta k}[1-\exp(i\Delta kx)], \qquad (3.9)$$

according to which the wave amplitude of the second harmonic does not remain constant but exhibits beats in space

$$|A_2|=\gamma\frac{|\sin(\Delta kx/2)|A_0^2}{\Delta k/2}. \qquad (3.10)$$

In the absence of dispersion, $\Delta k=0$, the amplitude of the second harmonic grows linearly with the distance (see Fig. 11)

$$|A_2|=\gamma A_0^2x. \qquad (3.11)$$

Due to the condition $|A_2|\ll A_0$ this equation is valid also for $\Delta k\neq0$ but $x\ll x_n$.

In the general case $\Delta k\neq0$ the second harmonic amplitude *increases monotonically within the interval* L_{coh} (Refs. 1–4)

$$L_{\text{coh}}=\frac{\pi}{\Delta k}=\frac{\pi}{|2k_1-k_2|}, \qquad (3.12)$$

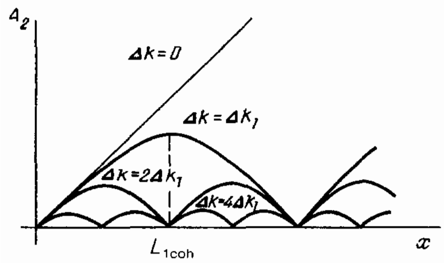

FIG. 11. Generation of the second harmonic for different dispersion properties of the medium.

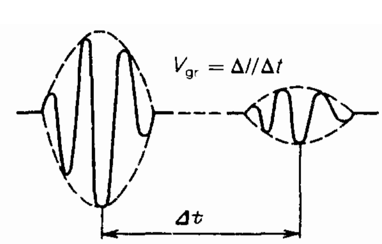

FIG. 13. The experimental method for the determination of the capillary wave group velocity.

where L_{coh} is the so-called "coherence length," and reaches the first maximum

$$|A_2|_{max} = \frac{2\gamma A_0^2}{\Delta k}. \tag{3.13}$$

The spatial period of beats is

$$\Delta_{2\omega} = 2L_{coh} = \frac{2\pi}{|2k_1 - k_2|} \tag{3.14}$$

(see Fig. 11).

The block diagram of the apparatus for the experimental investigation of capillary waves is shown in Fig. 12. Surface waves are generated in small bath *1* by the sharp edge of the light aluminum plate *2* firmly attached to the electrodynamic transducer *3*. The electromagnetic oscillations are generated both in the continuous and the pulsed regimes by the generator *4* in the frequency range 40–200 Hz. The water depth in the bath of $h \simeq 5$ cm was sufficient to justify neglecting the influence of the bottom on the propagation of waves in the frequency range of 40–200 Hz. A 5V constant voltage battery is attached to the receiving circuit which contains the adjusting resistor R_0, the thick copper plate *5* on the bath bottom and the thin gold electrode *6* (Fig. 12). The changes in the depth to which the electrode is submerged due to water surface oscillations result in oscillations of the receiving circuit resistance. The alternating voltage across R_0 which is proportional to the surface wave amplitude is selected and amplified by the selective micro voltmeter *7* and then the output signal is applied to the Y input of the oscilloscope *8*. During the experiment the receiving device travels in the direction of the surface wave propagation and its displacement is measured with a micrometer.

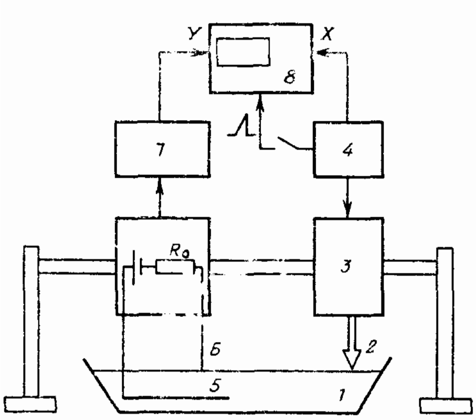

FIG. 12. Block diagram of the experimental apparatus for the investigation of capillary waves on a water surface.

This experimental device is suitable for the investigation of V_{ph} and V_{gr} dispersions as well as the second harmonic generation process. When measuring the $V_{ph}(f)$ dependence a continuous alternating electric voltage from the generator *4* is applied to the transducer *3* and to the X input of the oscilloscope. The phase difference between the initial and the received signals is measured by using the ellipsoidal Lissajoux patterns. The distance between two closest points of the receiving device at which the Lissajoux patterns had the same shape is equal to the wavelength λ that corresponds to $V_{ph} = f\lambda$. Making measurements at different frequencies one obtains the dispersion curve $V_{ph}(f)$ in the frequency range $f = 40$–200 Hz.

In order to measure V_{gr} the continuous regime of generation is changed to the pulsed one. The oscilloscope is synchronized by an external rectangular pulse which is also used for the electric signal modulation. Due to strong dispersion the initial rectangular wave packet is transformed into a Gaussian one. Measurement with the oscilloscope of the time shift Δt of the maximum of the wave packet caused by the spatial shift Δl of the receiving system allows one to estimate $V_{gr}(f) = \Delta l / \Delta t$ (see Fig. 13).

The experimental dependences $V_{ph}(f)$ and $V_{gr}(f)$ were compared with the theoretical ones. Experimental values appeared to be less then V_{ph} and V_{gr} from Eq. (3.3) because of the smaller value of σ of nondistilled water. In addition the air dust absorption by the water surface and the products of electrolysis in the receiving device also decreased the value of σ.

The continuous regime of generation mentioned above is used for the measurement of the second harmonic amplitude. The selective micro voltmeter is tuned to double the frequency of generation. The fine tuning of the receiving system is carried out using the optimal "figure of eight" Lissajoux pattern on the oscilloscope screen.

The monotonic increase of the value of A_2 was observed up to the distance L_{coh} between the transducer and the receiver, then space beats of A_2 were observed (See Fig. 11). Students measured the experimental $\Delta_{2\omega}$ value which was compared with the estimated value from Eq. (3.14).

CONCLUSION

The three practical laboratory exercises described in this paper are associated with nonlinear phenomena that in our opinion are the most interesting ones. Students graduating in radio physics study the modern experimental method of nonlinear acoustics when working on these practical exercises.

All the experimental set-ups are based on commercially produced type blocks. Their reliability was confirmed during several years of exploitation in the Physics Department of Moscow State University. The second exercise was carried out using personal computers both of domestic production (DUK-2, 3, "Électronika-60," and Iskra 1130) as well as of foreign production (compatible with IBM PC).

More detailed information is available from the Acoustics Section of the Physics Department of the M. V. Lomonosov Moscow State University.

We thank Prof. I. A. Yakovlev for his interest in this article and for helpful and stimulating discussion of it.

[1)] The author of this exercise is V. A. Burov.
[2)] The authors of this exercise are O. V. Rudenko and Yu. R. Lapidus.
[3)] The authors of this exercise are B. B. Voronov and A. I. Korobov.

[1] M. B. Vinogradova, O. V. Rudenko, and A. P. Sukhorukov, *Wave Theory* (in Russian), Nauka, M., 1990.
[2] L. K. Zarembo and V. A. Krasil'nikov, *Introduction to Nonlinear Acoustics* (in Russian), Nauka, M., 1966.
[3] V. A. Krasil'nikov and V. V. Krylov, *Introduction to Physical Acoustics* (in Russian), Nauka, M., 1984.
[4] O. V. Rudenko and S. I. Soluyan, *Theoretical Foundations of Nonlinear Acoustics* Plenum Publishing, N.Y., 1977. [Russ. original, Nauka, M., 1975].
[5] R. T. Beyer, *Nonlinear Acoustics. Naval Ship Systems Command*, 1974.
[6] B. K. Novikov, O. V. Rudenko, and V. I. Timoshenko, *Nonlinear Underwater Acoustics*, American Inst. of Physics, N.Y., 1987. [Russ. original Sudostroenie, L., 1981].
[7] F. Zernike and J. E. Midwinter, *Applied Nonlinear Optics*, Wiley, N.Y., 1973. [Russ. transl. Mir, M., 1976].
[8] K. A. Naugolinykh and L. A. Ostrovsky, *Nonlinear Wave Processes in Acoustics*, Cambridge Univ. Press, 1992. [Russ. Original, Nauka, M., 1990].
[9] N. S. Bakhvalov, Ya. M. Zhileĭkin, and E. A. Zabolot-skaya, *Nonlinear Theory of Sound Beams* (in Russian) Nauka, M., 1982.
[10] Yu. R. Lapidus and O. V. Rudenko, Akust. Zh. **30**, 797 (1984) [Sov. Phys. Acoust. **30**, 473 (1984)].

English text (differing in minor respects from the Russian text in Usp. Fiz. Nauk) was supplied by the authors.